Molecular dynamics analysis of the dipole moment and conformational properties of 2-(acetyloxy)ethyl-2-(2-naphthyl)acetate

Patricia Saez-Torres,[a] Maria P. Tarazona,[b] Enrique Saiz,[b] Evaristo Riande *,[a] and Julio Guzmán[a]

[a] *Instituto de Ciencia y Tecnología de Polímeros (CSIC), 28006-Madrid, Spain*
[b] *Departamento de Química Física, Universidad de Alcalá, 28871 Alcalá de Henares, Spain*

A sample of 2-(acetyloxy)ethyl-2-(2-naphthyl)acetate (ANA), model compound of the side group of poly(2-{[2-(2-naphthyl)-acetyl]oxy}ethyl acrylate) (PNAEA), has been synthesized and its mean-squared dipole moment measured in dioxane solutions at 30 °C, providing an experimental result of $\langle\mu^2\rangle = 5.28$ D^2. Molecular dynamics simulations, performed with the Amber force field, the DL_POLY package and the charge distribution provided by MOPAC, gives a theoretical value $\langle\mu^2\rangle = 5.69$ D^2, in good agreement with experience. The analysis of the MD trajectories indicates that the preferred orientations for the C^{ar}–CH$_2$ bond are those in which the plane defined by the pair of bonds C^{ar}–CH$_2$–C* is roughly perpendicular to the aromatic group (*i.e.* $\varphi \approx \pm 90°$) while *trans* orientation of the CH$_2$–C* bond is strongly disfavoured (by *ca.* 1.5 kcal mol^{-1}) *versus gauche*. In the O–CH$_2$–CH$_2$–O segment, the O–CH$_2$ bonds show a strong preference for *trans* while CH$_2$–CH$_2$ prefers *gauche* and does not require any kind of adjustment *a posteriori* to account for the so called '*gauche* effect'. Thus, the first-order conformational energies representing the stability of *gauche versus trans* are $E_\sigma \approx 1.2$, $E_{\sigma 1} \approx -0.9$ kcal mol^{-1} respectively for O–CH$_2$ and CH$_2$–CH$_2$. Second-order interactions E_ω and E_γ respectively controlling the stability of opposite (*i.e.* $g^\pm g^\mp$) and identical (*i.e.* $g^\pm g^\pm$) combinations of *gauche* states over the pair of bonds O–CH$_2$–CH$_2$ are both negative (*ca.* $E_\omega \approx -1$, $E_\gamma \approx -0.6$ kcal mol^{-1}). Values of the mean-squared dipole moment computed by adding contributions produced by two ester groups with this set of conformational energies are in very good agreement with the results obtained by the actual MD simulations.

Introduction

Dielectric relaxation spectra of glass-forming liquids present in the frequency domain, and just above their glass-liquid transition temperatures, a prominent absorption called α relaxation, followed by a fast and relatively weak process called β relaxation. An increase in temperature shifts both relaxations to higher frequencies, and as a consequence of the high activation energy of the α relaxation, a temperature can be reached at which both relaxations merge together forming the αβ relaxation.[1] The normalized αβ relaxation response function in the time domain exhibits at short times a relaxation process followed by a much more extended time regime in which the relaxation displays a Kohlrausch–Williams–Watts (KWW) stretched exponential decay given by[2,3] eqn. (1) where $0 < \beta \leqslant 1$ and $\tau(T)$

$$g(t) = \exp\left[-\left(\frac{t}{\tau(T)}\right)^{\beta}\right] \qquad (1)$$

is the mean relaxation time whose value is given by the area under the $g(t)$ curve along the positive time axis. The temperature dependence of τ in the vicinity of the glass transition temperature is described by the Vogel–Fulcher–Tammann–Hesse (VTHF) eqn. (2)[4–6] in which m and T_∞ are believed to be

$$\tau = A\exp\left[\frac{m}{T - T_\infty}\right] \qquad (2)$$

related, respectively, to the fractional free volume and to the Kauzmann temperature,[7,8] *i.e.* the temperature at which the conformational entropy vanishes. Transformation of the decay function from the time to the frequency domain allows the evaluation of the strength of the α relaxation process defined as $\Delta\varepsilon_\alpha = \varepsilon_0 - \varepsilon_\infty$, where ε_0 and ε_∞ represent, respectively, the relative permittivity at 0 and ∞ frequencies. In most cases the relaxation strength of the β process is negligible compared with that of the α relaxation and the value of $\Delta\varepsilon_\alpha$ can directly be obtained from the mean-square dipole moment $\langle\mu^2\rangle$ of the compounds by using Onsager[9] type expressions such as the Fröhlich equation.[10,11] The value of $\langle\mu^2\rangle$ can be computed by either assigning dipoles to bonds or groups of bonds and averaging the square of the vector sum for all the available conformations or from the trajectories of the dipole moment in the conformational space.[12–16] In the latter case this gives eqn. (3), where $\mu(t_i)$ is the

$$\langle\mu^2\rangle = \langle\boldsymbol{\mu}(t)\cdot\boldsymbol{\mu}(t)\rangle = \frac{1}{n}\sum_{i=1}^{n}\mu^2(t_i) \qquad (3)$$

dipole moment of the molecule at time t_i in the trajectory, and n is large enough as to make certain that the molecule visits all the conformational space.

This latter approach was used in the evaluation of the mean-square dipole moment of 2-(acetyloxy)ethyl-2-(2-naphthyl)-acetate (ANA), model compound of the side group of poly(2-{[2-(2-naphthyl)-acetyl]oxy}ethyl acrylate) (PNAEA), carried out in this work. Hydrolysis of both the model compound and the polymer[17,18] gives the naphthalene acetic acid, a compound widely used as a plant growth regulator. An important issue in the study of the conformational characteristics of model compounds containing the OCH$_2$–CH$_2$O moiety in their structure, as occurs in ANA, is that the rotational states population about CH$_2$–CH$_2$ bonds present a *gauche* effect, *i.e.* the experimental value of the energy of the *gauche* states with respect to the alternative *trans* states is significantly lower than that obtained by using semiempirical potential functions or semiempirical quantum mechanics methods.[19–21] The *gauche* effect expressed in terms of the difference between the experimental and calculated values of the energy of *gauche* states is *ca.* 1 kcal mol^{-1} for CH$_2$–CH$_2$ bonds in 1,2-dimethoxyethane (CH$_3$–OCH$_2$–CH$_2$–OCH$_3$).[20] Therefore, it is tempting to investigate how the two ester groups flanking the CH$_2$–CH$_2$ bond in 2-(acetyloxy)ethyl-2-(2-naphthyl)acetate (ANA) may affect the *gauche* population about this bond.

This study forms part of a more general study whose object-

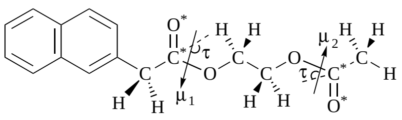

Fig. 1 A schematic sketch of the 2-(acetyloxy)ethyl-2-(2-naphthyl)-acetate (ANA) molecule shown in its planar all *trans* conformation for which the rotatable bonds on the acyclic residue were set to be $\varphi = 180°$. Dipole moments of the two ester groups are represented by arrows pointing from negative to positive centres of charges.

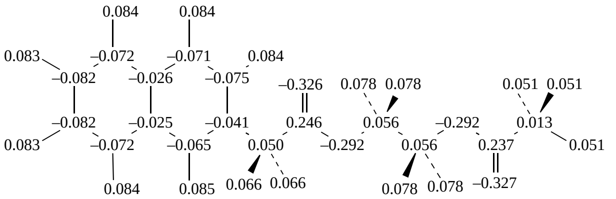

Fig. 2 Partial charges, in electron units, assigned to each atom of the 2-(acetyloxy)ethyl-2-(2-naphthyl)acetate (ANA) molecule with the MOPAC program and the AM1 procedure

ive is to investigate how the mobility of the side groups affects the mean-square dipole moment of acrylic polymers. This study will be extended in a further work to the simulation of the dielectric α relaxations of both the model compound ANA and the polymer PNAEA.

Molecular dynamics calculations

The structure of the ANA molecule is shown in Fig. 1 where all the rotating bonds on the molecule have been drawn in their planar *trans* conformation for which the value of the rotational angles φ were set to be 180°. Dipole moments of the molecule were calculated by means of partial charges assigned to each atom. They were computed with the MOPAC program and the AM1 procedure.[22] Fig. 2 indicates the charges assigned to each atom.

Molecular dynamic (MD) simulations were performed at $T = 300$ K with the DL_POLY package[23] employing the Amber force field.[24–26] A time step $\delta = 1$ fs (*i.e.* 10^{-15} s) was used for the integration cycle that was repeated 10^7 times to cover a total time span of 10 ns (*i.e.* 10^{-8} s) for the whole simulation. Conformations obtained after each 1000 steps were recorded, thus providing a total of 10^4 conformations for posterior analysis. The geometry of the molecule was first optimized with respect to all bond lengths, bond angles and rotations by minimizing its conformational energy. This optimized geometry was then used as starting point for the MD simulation whose first assignment was to warm up the molecule from 0 K to the working temperature with increments of 20 K and allowing a relaxation period of 500 fs at each intermediate temperature. Once the sample was stabilized at 300 K, the collection of data started. No scaling of the 1–4 interactions was performed. The Coulombic term of the potential energy was computed as the sum of pairwise interactions according to eqn. (4), where E_{ij} indicates the

$$E_{ij} = 332 \frac{q_i q_j}{\varepsilon r_{ij}} \tag{4}$$

interaction between atoms i and j that are separated a distance r_{ij} and whose partial charges are q_i and q_j. The numerical constant 332 renders E_{ij} in kcal mol^{-1} when charges are given in electron units and distances in Å. A value $\varepsilon = 4$ was used for the relative permittivity of the system.

The temperature of the sample was controlled by scaling the atomic velocities after each integration cycle with a factor λ defined in eqn. (5), where T_0 represents the working temperature (*i.e.* $T_0 = 300$ K in the present work) while T_i indicates the temperature evaluated with the atomic velocities after step i. The damping factor was set to $d = 1000$ fs. This is a rather high value for a damping factor, but it gently forces T_i towards the target temperature, thus ensuring that the averaged value for the whole simulation matches T_0, and, at the same time, allows relatively high thermal fluctuations that facilitate the passage over the rotational barriers.

$$\lambda_i = \left[1 + \left(\frac{\delta}{2d}\right)\left(\frac{T_0}{T_i} - 1\right)\right]^{\frac{1}{2}} \tag{5}$$

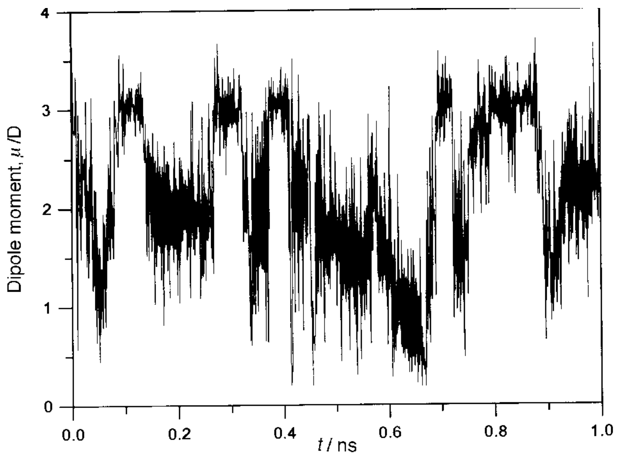

Fig. 3 Dipole moment of the sample, μ, as a function of time during first ns of the simulation. Averaged results are: $\langle|\mu|\rangle = 2.25$ D, $\langle\mu^2\rangle = 5.69$ D^2.

Table 1 Averaged positions, probabilities and relative energies of the rotational isomers for rotatable bonds of the acyclic residue of the ANA molecule

Bond	State	$\langle\varphi\rangle$/°	Probability at 300 K	E (relative)/kcal mol^{-1}
C^{ar}–CH_2	perpen.	86.6	0.500	0.00
	perpen.	272.6	0.500	0.00
CH_2–C*	*trans*	178.6	0.040	0.00
	gauche	294.1	0.480	−1.48
	gauche$^-$	66.5	0.480	−1.48
O–CH_2	*trans*	179.8	0.618	0.00
	gauche	285.3	0.191	0.70
	gauche$^-$	76.4	0.191	0.70
CH_2–CH_2	*trans*	179.4	0.070	0.00
	gauche	295.0	0.465	−1.13
	gauche$^-$	64.5	0.465	−1.13

Fig. 3 represents the time evolution of the dipole moment μ during the first ns of the simulation. The instantaneous values oscillate between a maximum of *ca.* 4 D and a minimum of roughly 0, while the averaged results for the whole simulation are $\langle|\mu|\rangle = 2.25$ D and $\langle\mu^2\rangle = 5.69$ D^2, this latter value being in good agreement with the experimental result, 5.28 D^2.

The probability distribution of each rotating bond on the acyclic fragment, taken as independent of its neighbours, was computed by counting how many times along the simulation the studied angle reached a given value with a tolerance of ±5⁰, (for instance, the results indicated for $\varphi = 40$ represent the fraction of conformations in which $35 < \varphi < 45$). The results are depicted in Figs. 4–6, while some more quantitative information is presented in Table 1 that summarizes the averaged positions, probabilities and relative energies of the rotational isomers for all these angles, excluding the O–C* which are always in *trans* and the final C*–CH_3 which is irrelevant.

As Fig. 4 indicates, the preferred states for bond C^{ar}–CH_2 are those in which the plane defined by the pair of bonds C^{ar}–CH_2–C* is roughly perpendicular to the aromatic group, *i.e.* $\varphi \approx 90$, 270°. The staggered orientations of this bond produce strong repulsions of the H atoms on the ring with the H of the CH_2 and the carbonyl O*. On the other hand, the *trans* orientation of the CH_2–C* bond is strongly disfavoured *versus*

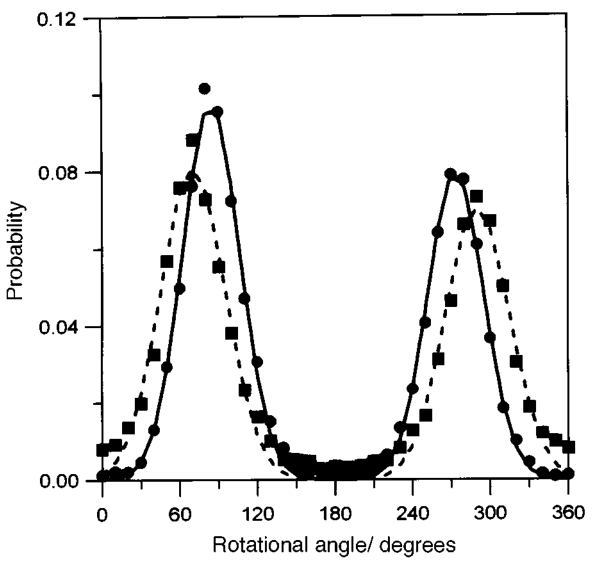

Fig. 4 Probability distributions for rotations over C^{ar}–CH_2 (—) and CH_2–C* (– – –) bonds. Points indicate the actual probabilities computed along the MD simulation while the lines represent least squares fittings and are drawn to show up the shape of the distributions.

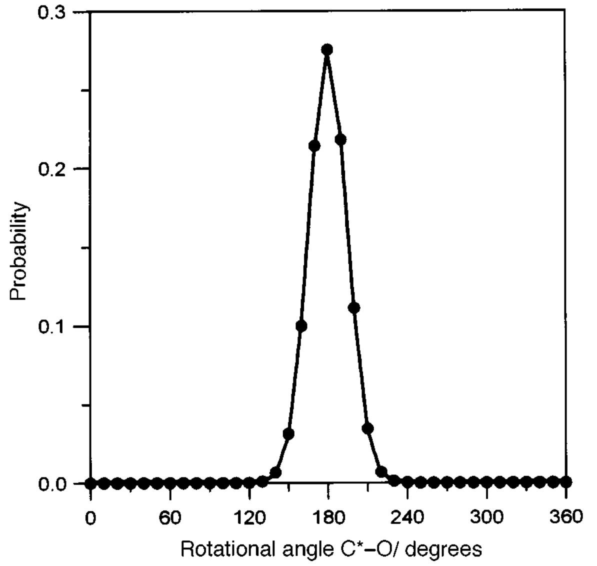

Fig. 5 Probability distributions for rotations over C*–O bonds. See legend for Fig. 4.

gauche (*i.e. gauche* is *ca.* 1.5 kcal mol^{-1} below *trans* according to Table 1). The reason for this difference lies in the interaction between the carbonyl O* and the C^{ar} attached to the acyclic residue that are separated *ca.* 2.6 and 3.0 Å, respectively, for *trans* and *gauche* orientations.

Fig. 5 shows the results obtained with the two equivalent C*–O bonds of the molecule for which *trans* is the only allowed orientation. Thus, even if they fluctuate along the MD simulation within a ±30° range, they never cross the barrier to the alternative *cis* conformation.

The analysis of the O–CH_2–CH_2–O segment, whose results are summarized in Fig. 6, is more interesting, since the relative orientation of these three bonds is the main feature that controls the value of the dipole moment for the whole molecule (see below). Our results indicate that *trans* is the preferred orientation for the O–CH_2 bonds, while CH_2–CH_2 prefers *gauche*, as was found before in the analysis of similar compounds employing a different procedure.[27] It is interesting to notice that in the present calculation the preference of bonds OCH_2–CH_2O for *gauche* states is not introduced *a posteriori* by means of a so-called *gauche effect* that has been invoked many times for the analysis of polyoxides.[21] The reason is that the Amber force field contains a better parametrization of this kind of bond, mainly as regards the intrinsic rotational barrier.

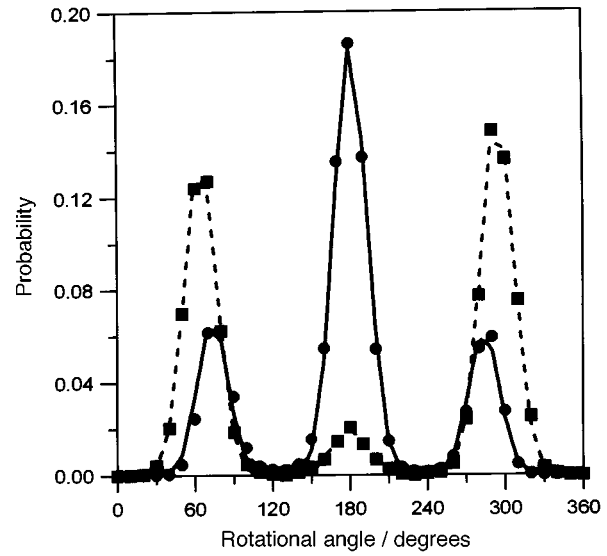

Fig. 6 Probability distributions for rotations over O–CH_2 (—) and CH_2–CH_2 (– – –) bonds. See legend for Fig. 4.

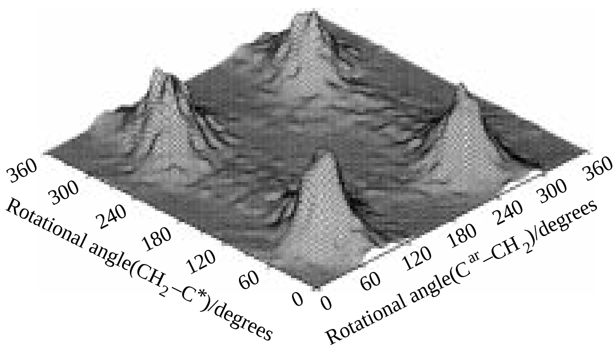

Fig. 7 Distribution of the *a priori* probabilities for the C^{ar}–CH_2–C* pair of bonds

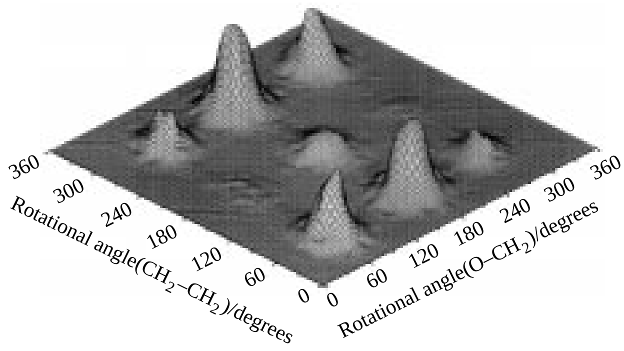

Fig. 8 Distribution of the *a priori* probabilities for the O–CH_2–CH_2 pair of bonds

The distributions of *a priori* probabilities for correlated pairs of bonds are represented in Fig. 7 for the pair of bonds C^{ar}–CH_2–C* and in Fig. 8 for O–CH_2–CH_2 and its mirror image CH_2–CH_2–O (with interchange of x and y axes for this last pair). Fig. 7 shows four roughly equivalent maxima, each one representing a probability of *ca.* 24%, at the combination of orientations $\varphi_1 = \pm 90°$ for bond C^{ar}–CH_2, $\varphi_2 = \pm 60°$ for CH_2–C*. However, the orientations placing CH_2–C* bond *trans* only represent a probability of *ca.* 4%. Thus, the information provided when this pair of bonds is taken to be correlated is about the same as that which could be obtained by the analysis of the same bonds taken independently.

The probabilities for the pair of bonds O–CH_2–CH_2, represented in Fig. 8, show two main maxima, each representing a

Table 2 Probabilities of occurrence (computed at $T = 300$ K), energies (in kcal mol^{-1}) relative to the all *trans* conformation, first- and second-order contributions to the conformational energies for the allowed conformations of the O–CH$_2$–CH$_2$–O segment of the ANA molecule. The last two columns were computed with the following values of conformational energies: $E_\sigma = 1.20$; $E_{\sigma 1} = -0.87$; $E_\omega = -0.13$; $E_\gamma = -0.57$ kcal mol^{-1}

	From MD			From contrib.	
States[a]	Prob.	E_{rel}	Contributions	Prob.	E_{rel}
ttt (1)	0.0420	0.00	0	0.0469	0.00
ttg (4)	0.0065	1.11	E_σ	0.0063	1.20
tgt (2)	0.1358	−0.70	$E_{\sigma 1}$	0.2018	−0.87
tgg (4)	0.0838	−0.41	$E_\sigma + E_{\sigma 1} + E_\gamma$	0.0701	−0.24
tgg^- (4)	0.0593	−0.21	$E_\sigma + E_{\sigma 1} + E_\omega$	0.0335	0.20
gtg (2)	0.0007	2.44	$2E_\sigma$	0.0008	2.40
gtg^- (2)	0.0009	2.29	$2E_\sigma$	0.0008	2.40
ggg (2)	0.0135	0.68	$2E_\sigma + E_{\sigma 1} + 2E_\gamma$	0.0244	0.39
ggg^- (4)	0.0129	0.70	$2E_\sigma + E_{\sigma 1} + E_\omega + E_\gamma$	0.0117	0.83
g^-g (2)	0.0031	1.55	$2E_\sigma + E_{\sigma 1} + 2E_\omega$	0.0057	1.27

[a] Symmetrically equivalent conformations listed below are not included in the body of the table for simplicity. The number of conformations represented by each one of those included is given in brackets. $ttg = ttg^- = gtt = g^-tt$, $tgt = tg^-t$, $tgg = tg^-g^- = ggt = g^-g^-t$, $tgg^- = tg^-g = g^-t = g^-gt$, $gtg = g^-tg^-$, $gtg^- = g^-tg$, $ggg = g^-g^-g^-$, $ggg^- = g^-g = g^-g^- = g^-g^-g^-$, $g^-g = g^-g^-$.

probability of *ca.* 0.25, for the *tg* and tg^- conformations [*i.e.* φ(O–CH$_2$) = 180°, φ(CH$_2$–CH$_2$) ≈ ±60°], which are a combination of the preferred states for both kind of bonds. The next pair of relevant maxima are *gg* and g^-g^-, each having a probability of *ca.* 0.14. The probability for each one of the combinations gg^- and g^-g is *ca.* 0.06. The conformations placing the second bond *trans* have low probabilities, thus *tt* amounts to *ca.* 0.06 while each of the remaining *gt* and g^-t possibilities that place both bonds in their disfavoured states have probabilities of *ca.* 0.02.

A more detailed analysis of the conformations adopted by the O–CH$_2$–CH$_2$–O segment is summarized in Table 2. The possible conformations adopted by these three bonds are collected in the first column, although only one of each possible series of symmetrically equivalent orientations is represented in order to simplify the Table. The multiplicity, *i.e.* the number of symmetrical conformations for each row, is given in brackets. The probabilities computed at $T = 300$ K for each conformation are given in the second column. They were obtained by counting how many conformations along the MD simulation placed simultaneously the three rotational angles in the desired orientations and averaging the results for each series of equivalent conformations. These probabilities were used to calculate conformational energies as $E_i = -RT \ln p_i$ where i represents each of the studied conformations. Values of these energies, normalized to give $E = 0$ for *ttt*, are collected in the third column.

The total energy of any given conformation is customarily separated into a sum of first- and second-order interactions. First-order interactions are those produced among pairs of atoms whose separation depends on just one rotational angle. In the present case, first-order interactions can be represented by two parameters, namely E_σ that represents the energy of *gauche* orientations relative to *trans* for the O–CH$_2$ bonds, and $E_{\sigma 1}$ that has the same meaning for the CH$_2$–CH$_2$ bond. Second-order interactions are those produced by pairs of atoms whose separation depend on two consecutive rotations and we represent by E_ω the interactions produced in pairs of different *gauche* states, *i.e.* gg^- or g^-g conformations and by E_γ the interactions raised in *gg* or g^-g^- orientations. The fourth column in Table 2 indicates the combination of these parameters required to represent each one of the conformations. The values of these contributions are assigned in such a way that they produce the best possible fitting of the actual conformational energies indicated in the previous column, and in this sense, the combination: $E_\sigma = 1.20$, $E_{\sigma 1} = -0.87$, $E_\omega = -0.13$, $E_\gamma = -0.57$ kcal mol^{-1} provides very good results, as shown in Table 2 whose last two columns were computed with these values of the conformational energies.

The values of the first-order parameters seem to be reasonable since they indicate that the O–CH$_2$ bonds prefer *trans* orientations while *gauche* are favoured in the case of CH$_2$–CH$_2$ bonds. However, the results obtained for the second-order interactions E_ω and E_γ are quite amazing because they are both negative, whereas in most polymeric systems E_ω is large and positive (in many cases E_ω is taken to be infinity thus forbidding the gg^- and g^-g conformations) while E_γ is usually set equal to zero (*i.e.* second-order interactions produced in *gg* and g^-g^- conformations are supposed to be rather weak). Nevertheless, some more recent analysis based on *ab initio* calculations provide negative values for these second-order energies.[28]

The reason for the present results is that the most important second-order interactions for the O–CH$_2$–CH$_2$ pair of bonds are produced by the O* on the first ester group and the O atom on the second CH$_2$O group. Taking into account that the C*–O bond is always close to *trans* (see Fig. 5), the O* atom lies in the plane defined by the C*–O–CH$_2$ pair of bonds and this fact makes the differences from g^-, g^-g to g, g^-g^- conformations to be much smaller than in polymers where the groups involved are for instance two CH$_2$. Thus, in the g^- orientation, the O* of the first ester and the O of the second one would be placed at a distance of *ca.* 1.7 Å if the molecule were in the undistorted geometry (*i.e.* all the rotations in the perfectly staggered positions and all bond lengths and bond angles in their main value). Such a short distance between these two atoms would produce a strong repulsion that should render a large and positive value of E_ω. However, it is quite easy to produce a noticeable increase in that distance through small adjustments of rotations and bond angles so that the interaction becomes attractive. On the other hand, the g conformation, in the undistorted geometry, places the first O* atom at a distance of 1.8 Å from one of the H atoms of the second CH$_2$ group, so that the situation is not too different from the previous case, in particular, this distance could also be increased by small adjustments producing a negative value of E_γ.

The most important contributions to the total dipole moment of this molecule come from the two ester groups, and since the orientation of the O–CH$_2$–CH$_2$–O segment controls the relative orientations of these two contributions and therefore their possible reinforcement or cancellation, it seems reasonable to presume that the dipole moment of the complete molecule will depend almost exclusively on the conformational characteristics of this segment. Some calculations were performed by adding the dipole moment of two ester groups (represented as μ_1 and μ_2 in Fig. 1). In these molecules[29] $\mu_1 = \mu_2 = 1.75$ D, and each dipole forms an angle $\tau = 121°$ with the respective C–C* bond.[30] The results obtained with different values of the conformational energies and location of the rotational isomers are summarized in Table 3. The first line in this Table contains the 'main set' of parameters, *i.e.* the values of energies indicated above and rotational isomers located at $\varphi(t, g^\pm) = 180°, \pm 45°$ for C–O bonds and 180°, ±55° for CH$_2$–CH$_2$, as suggested by Fig. 7

Table 3 Dipole moments of the ANA molecule computed at 300 K by adding two contributions arising from the ester groups, ($\mu_1 = \mu_2 = 1.75$ D, $\tau = 121°$, see Fig. 1), with several combinations of conformational energies (in kcal mol^{-1}), and location of *gauche* rotational isomers (*trans*, were always kept in 180°)

E_σ	$E_{\sigma 1}$	E_ω	E_γ	φ_g(C–O)	φ_g(C–C)	$\langle\mu^2\rangle$/D^2
1.20	−0.87	−0.13	−0.57	±45	±55	5.73
1.00	−0.87	−0.13	−0.57	±45	±55	5.78
1.40	−0.87	−0.13	−0.57	±45	±55	5.62
1.20	−0.67	−0.13	−0.57	±45	±55	5.62
1.20	−1.07	−0.13	−0.57	±45	±55	5.81
1.20	−0.87	−0.13	−0.57	±45	±55	6.09
1.20	−0.87	+0.07	−0.57	±45	±55	5.44
1.20	−0.87	−0.13	−0.77	±45	±55	5.45
1.20	−0.87	−0.13	−0.37	±45	±55	5.93
1.20	−0.87	−0.13	−0.57	±40	±55	5.65
1.20	−0.87	−0.13	−0.57	±50	±55	5.81
1.20	−0.87	−0.13	−0.57	±45	±50	5.51
1.20	−0.87	−0.13	−0.57	±45	±60	5.94

and Table 1 which indicate that *trans* conformations are located at 180° while *gauche* are displaced by *ca.* Δ(C–O) ≈ 15°, Δ(CH_2–CH_2) ≈ 5° from the perfectly staggered positions. This main set of parameters gives $\langle\mu^2\rangle = 5.73$ D^2, in excellent agreement with the result obtained from the actual MD simulation. The remaining lines on Table 3 indicate the variation produced in $\langle\mu^2\rangle$ by small modifications to the conformational parameters. It is interesting to note that the total dipole moment is more sensitive to the second-order energies E_ω and E_γ than to the first-order parameters E_σ and $E_{\sigma 1}$. The reason is that tgg^-, g^-g and all their symmetrically equivalent conformations, which are controlled by E_ω, produce the highest total dipole moment so that $\langle\mu^2\rangle$ increases with increasing value of E_ω. On the contrary, ggg and $g^-g^-g^-$, which are controlled by E_γ, are, together with *ttt*, the orientations of lowest polarity so that $\langle\mu^2\rangle$ decreases when the value of γ increases. It is also noteworthy that the dipole moment of the molecule is rather sensitive to the location of *gauche* states, especially for the CH_2–CH_2 bond, with $\langle\mu^2\rangle$ increasing when both states approach their staggered positions (*i.e.* with decreasing values of the Δ displacement), where μ_1 and μ_2 contributions are roughly parallel for conformations such as tgg^-.

Discussion

The results presented in this analysis, as well as many others reported elsewhere, show that MD simulations give a good account of the polarity of molecules. The use of MD simulations in the determination of dipole moments has the enormous advantage over other more traditional procedures that it does not require *a priori* knowledge of the polarity of molecular compounds containing groups of atoms with polarity similar to that of the molecule under investigation. At first sight, MD simulations do not seem suitable to predict the polarity of molecules, such as polymers, with a high number of internal degrees of freedom. However, contributions of cross correlation terms to the polarity of molecular chains fall rather sharply as the distance between dipoles increases, so that MD simulations performed on relatively short chains can give a good account of the polarity of larger ones.[21]

The value of 1.2 kcal mol^{-1} obtained in this work for the conformational energy of *gauche* states about CH_2–O bonds of the ester residue of ANA is nearly 1 kcal mol^{-1} higher than the value of this quantity currently used in the analysis of the conformational properties of polyesters.[19,21] It should be pointed out, however, that this energy has a relatively low effect on the polarity of the molecule. As occurs in polyoxyethylene (POE), where the orientation of the dipoles of two consecutive repeating units are separated by one CH_2–CH_2 bond, the polarity of ANA is very sensitive to the conformational energy of that bond. In the case of POE *gauche* states about CH_2–CH_2 bonds give rise to strong repulsive interactions between the negative residual charges of two oxygen atoms. As a consequence of the Coulombic contributions, most semiempirical calculations reported to date for the energy of *gauche* states about CH_2–CH_2 bonds in 1,2-dimethoxyethane and POE suggest that the energy $E_{\sigma 1}$ of these states is *ca.* 0.5 kcal mol^{-1} above that of the alternative *trans* state. However, in order to reproduce the dipole moment of 1,2-dimethoxyethane and both the dipole moments and the unperturbed dimensions of POE it is necessary to assume that $E_{\sigma 1}$ is *ca.* 0.5 kcal mol^{-1} below the energy of the corresponding *trans* state.[19,20] The difference between calculated and experimental conformational energies is commonly called the *gauche* effect in the literature. This effect appears in the cases in which electronegative atoms (O, S, Cl, *etc.*) intervene in the first-order interactions. Therefore, the rather good agreement between the value of $E_{\sigma 1}$ and the value of this energy in both 1,2-dimethoxyethane and POE is remarkable despite the fact that in the former case rather strong repulsive Coulombic interactions also intervene. The value of $E_{\sigma 1}$ is also in very good agreement with that found by NMR techniques for the energy of *gauche* states about CH_2–CH_2 bonds of molecular compounds which give rise to interactions between an oxygen atom of an ester group and an oxygen atom of an ether group.[31]

In view of these results one can conclude that the potential energy surfaces calculated by using the Amber force field give a good account of the experimental values of the rotational energies about CH_2–CH_2 bonds which produce first-order O···O interactions without the need to invoke a *gauche* effect *a posteriori*, as is commonly made. Most of the force fields, though conveniently parametrized for conformational analysis of paraffins, polyethylene and polyolefines, fail for polar molecules. In the latter case, the use of the Amber force field seems more convenient to obtain the true values of conformational energies.

Experimental

Synthesis and characterization of 2-(acetyloxy)ethyl-2-(2-naphthyl)acetate

Esterification of naphthyl acetic (NAA) acid with ethylene glycol (EG) (molar ratio NAA/EG = 35/88) was carried out in refluxing toluene, under a nitrogen atmosphere, using *p*-toluenesulfonic acid as catalyst. The reaction was allowed to proceed for 24 h utilizing a Dean–Stark distillation trap to separate the water formed in the esterification process. The solvent was eliminated at reduced pressure and the monoester, 2-hydroxyethyl-2-(2-naphthyl)acetate (HNA), and diester, ethylene glycol dinaphthyl acetate (EGDA), formed in the reaction were separated in successive silica gel columns using the following eluents: hexane–ethyl acetate (3:1), hexane–ethyl acetate (2:1) and hexane–ethyl acetate (1:1).

Characterization of the monoester: ^{1}H NMR (200 MHz) ($CDCl_3$): δ 7.85–7.15 (m, 7H, protons of the naphthyl group), 4.05 (m, 2H, $-COO-CH_2-CH_2-OH$), 3.95 (s, 2H, naphthyl-CH_2-), 3.80 (s, 1H, OH), 3.50 ppm (t, 2H, $-CH_2-OH$).

^{13}C NMR (50.4 MHz) ($CDCl_3$): δ 171.8 (–COO–), 133.8–123.6 (carbon atoms of the naphthyl group), 66.5 ($-O-CH_2-CH_2-OH$), 61.0 ($-O-CH_2-CH_2-OH$), 39.0 ppm (naphthyl–CH_2-).

Acetyl chloride was added dropwise to a solution of HNA in benzene with stirring. Triethylamine, Et_3N, was present in the solution to neutralize the HCl formed. The reaction medium was washed three times with water and the organic phase was separated. In the same way, the aqueous phase was treated with benzene to extract the organic product present in this phase, and the washings were added to the first set. The organic phase was dried with sodium sulfate, filtered and the solvent separated under reduced pressure. The diesterified product, 2-(acetyloxy)-

ethyl-2-(2-naphthyl)acetate, was purified using a silicagel column and hexane–ethyl acetate (4 : 1) as eluent.

Characterization of ANA: ^{1}H NMR (200 MHz) ([^{2}H$_6$]-DMSO): δ 7.96–7.44 (m, 7H, protons of the naphthyl group), 4.30–4.16 (m, 6H, $-CH_2-$), 1.93 ppm (s, 3H, $-CH_3$).

^{13}C NMR (50.4 MHz) ([^{2}H$_6$]DMSO): δ 171.1, 170.1 (carbonyl groups), 133.3–123.8 (carbon atoms of the naphthyl group), 62.2, 61.8 ($O-CH_2-CH_2-O$), 37.9 (naphthyl$-CH_2-$), 20.4 ppm ($-CH_3$).

Dipole moment of 2-(acetyloxy)ethyl-2-(2-naphthyl)acetate

Static relative permittivities ε of solutions of ANA in benzene were measured, at 30 °C and at 10 kHz, with a capacitance bridge (General Radio, type 1620 A) coupled with a three-terminal cell. By plotting the increments of the relative permittivity of the solutions with respect to that of the solvent against the weight fraction of solute, w, a straight line was obtained whose slope, $d\varepsilon/dw$, is proportional to the total polarization of the solute. In the same way, increments of the index of refraction of the solution, n, with respect to that of the solvent were measured with a differential refractometer (Chromatix, Inc.). The plot of these increments *vs.* w gave a straight line whose slope, dn/dw, is proportional to the electronic polarization. The atomic polarization is in most cases less than 10% of the electronic polarization and in this case was considered negligible. The value of the mean-square dipole moment, $\langle \mu^2 \rangle$, of ANA was determined by means of the method of Guggenheim

$$\langle \mu^2 \rangle = \frac{27 k_B M T}{4\pi \rho N_A (\varepsilon_1 + 2)^2}\left[\frac{d\varepsilon}{dw} - 2n_1 \frac{dn}{dw}\right] \qquad (6)$$

and Smith,[32,33] eqn. (6), where k_B and N_A are, respectively, the Boltzmann's constant and Avogadro's number, M is the molecular weight of the solute and ρ is the density of the solvent. The subindex 1 in eqn. (6) refers to the property of the solvent. The experimental values of $d\varepsilon/dw$ and dn/dw at 30 °C were 2.18 and 0.046. By substituting these results into eqn. (4) one determines that the mean-square dipole moment of ANA in vacuum is 5.28 D^2. The uncertainty of this value was estimated to be *ca.* 2.5%.

Acknowledgements

This work was supported by the DGICYT through Grants PB94-0364 and PB 95-0134-C02-01.

References

1 G. Williams, *Dielectric Spectroscopy of Amorphous Polymer Systems: The Modern Approaches*, in *Keynote Lectures in Selected Topics of Polymer Science*, ed. E. Riande, CSIC, Madrid, 1995.
2 R. Kohlrausch, *Ann. Phys.*, 1847, **12**(3), 3931.
3 G. Williams and D. C. Watts, *Trans. Faraday Soc.*, 1970, **66**, 80.
4 H. Vogel, *Z. Phys.*, 1921, **22**, 645.
5 G. S. Fulcher, *J. Am. Ceram. Soc.*, 1925, **8**, 339.
6 G. Tammann and W. Z. Hesse, *Anorg. Allgem. Chem.*, 1926, **156**, 245.
7 F. H. Stillinger, *Science*, 1995, **267**, 1935.
8 K. Kauzmann, *Chem. Rev.*, 1948, **43**, 219.
9 L. Onsager, *J. Am. Chem. Soc.*, 1936, **58**, 1486.
10 H. Fröhlich, *Trans. Faraday Soc.*, 1948, **44**, 238.
11 H. Fröhlich, *Theory of Dielectrics*, Oxford University Press, London, 1958.
12 R. C. Nunes, M. R. Pinto, E. Saiz and E. Riande, *Macromolecules*, 1995, **28**, 211.
13 E. Saiz, C. Alvarez, E. Riande, M.R. Pinto and C. Salom, *J. Chem. Phys.*, 1996, **105**, 8266.
14 E. Saiz and E. Riande, *J. Chem. Phys.*, 1995, **103**, 3832.
15 E. Saiz, E. Riande, J. Guzmán and M. T. Iglesias, *J. Phys. Chem.*, 1996, **100**, 3818.
16 E. Saiz, J. Guzmán, M. T. Iglesias and E. Riande, *J. Phys. Chem.*, 1996, **100**, 18 345.
17 C. L. McCormick and K. Kim, *J. Controll. Release*, 1988, **7**, 101.
18 C. L. McCormick, *Ann. N.Y. Acad. Sci.*, 1985, **76**, 446.
19 P. J. Flory, *Statistical Mechanics of Chain Molecules*, Interscience, New York, 1969.
20 A. Abe and J. E. Mark, *J. Am. Chem. Soc.*, 1976, **98**, 6468.
21 E. Riande and E. Saiz, *Dipole Moments and Birefringence of Polymers*, Prentice Hall, Englewood Cliffs, NJ, 1992.
22 QCPE, Department of Chemistry, Indiana University, Bloomington, IN, 47405.
23 T. R. Forester and W. Smith, *DL_POLY* (Ver. 2.0), Daresbury Laboratory, Daresbury, Warrington, WA4 4AD, England.
24 S. J. Weiner, P. A. Kollman, D. A. Case, U. C. Singh, C. Ghio, G. Alagona, S. Profeta Jr. and P. Weiner, *J. Am. Chem. Soc.*, 1984, **106**, 765.
25 S. J. Weiner, P. A. Kollman, D. T. Nguyen and D. A. Case, *J. Comput. Chem.*, 1986, **7**, 230.
26 S. W. Homas, *Biochemistry*, 1990, **29**, 9110.
27 F. Mendicuti, M. M. Rodrigo, M. P. Tarazona and E. Saiz, *Macromolecules*, 1990, **23**, 1139.
28 G. D. Smith, D. Y. Yoon and R. L. Jaffe, *Macromolecules*, 1993, **26**, 5213.
29 A. L. McClellan, *Tables of Experimental Dipole Moments*, Freeman, San Francisco, 1963, Vol. I; Rahara Enterprises, El Cerrito, Cal, 1974, Vol. II; 1989, Vol III.
30 E. Saiz, J. P. Hummel, P. J. Flory and M. Plavsic, *J. Phys. Chem.*, 1981, **85**, 3211.
31 J. San Román, J. Guzmán, E. Riande, J. Santoro and M. Rico, *Macromolecules*, 1982, **15**, 609.
32 E. A. Guggenheim, *Trans. Faraday Soc.*, 1949, **45**, 714.
33 J. W. Smith, *Trans. Faraday Soc.*, 1950, **46**, 394.

Paper 7/05566H
Received 31*st July* 1997
Accepted 5*th September* 1997